Fibers and Polymers 2012, Vol.13, No.7, 823-830 DOI 10.1007/s12221-012-0823-3

Fabrication of Electrospun Poly L-lactide and Curcumin Loaded Poly L-lactide Nanofibers for Drug Delivery

Elakkiya Thangaraju, Natarajan Thirupathur Srinivasan[1], Ramadhar Kumar[2], Praveen Kumar Sehgal[2], and Sheeja Rajiv*

Department of Chemistry, Anna University, Tamilnadu 600 025, India
[1]*Department of Physics, Indian Institute of Technology Madras (IITM), Tamilnadu 600 036, India*
[2]*Department of Bioproducts, Central Leather Research Institute (CLRI), Adyar, Tamilnadu 600 020, India*
(Received October 10, 2011; Revised November 24, 2011; Accepted November 25, 2011)

Abstract: The present work reports the preparation of Poly L-Lactide (PLLA) and Curcumin loaded Poly L-Lactide (C-PLLA) nanofibers by electrospinning. A series of PLLA solution (12 wt %) and C-PLLA (12 wt % PLLA) solution containing Curcumin (0.5 wt % and 1 wt %)) were electrospun into nanofibers. SEM images showed the average diameter of PLLA and C-PLLA in the range of 50-200 nm. The TEM images showed the dispersion of Curcumin on C-PLLA nanofibers. The XRD pattern indicated decreases of crystallinity with the increase in the amount of Curcumin. The characteristic peak of Curcumin was confirmed by FTIR. The TGA results showed the degradation of PLLA and C-PLLA close to 300 ºC. The percentage porosity and the contact angle of PLLA were found to be 90.2 % and 115±3 º with deionised water, respectively. The water uptake percentage was found to be 17.6 %. The percentage cumulative release of Curcumin at the end of 8th day for 0.5 and 1.0 wt % formulations was 81.4±1.3 and 86.7±1.7 % respectively. The *in-vitro* biological cytotoxicity studies were performed using C6 glioma cells and NIH 3T3 fibroblast by MTT assay and SEM analysis.

Keywords: Electrospinning, Nanofibers, PLLA, Curcumin, Drug delivery

Introduction

Electrospinning of polymer solutions lead to the formation of nano sized fibers which mimic the extracellular matrix and can be used as scaffolds with high surface area and small pore sizes with a certain level of molecular orientation suitable for drug release application [1-3]. Poly L-Lactide (PLLA) is one of the best defined biocompatible polymers with controlled degradation rate (mass and volume loss with respect to time) on the basis of crystallinity and hydrolytic attack on the ester bonds. Further the degraded monomers in PLLA (i.e.) lactic acid is easily metabolized and removed from the body by normal metabolic pathways thus making it a successful candidate for drug delivery. Curcumin is a safe and established drug under clinical trials that induces apoptosis in human cancer cell lines derived from lung, breast and pancreatic carcinoma [4,5]. Curcumin (diferuloyl methane) is a naturally occurring phenolic derivative obtained from the rhizome of turmeric (Curcuma longa L), with an ability to scavenge free radicals and inhibit inflammation [6,7]. In addition to the direct free radical scavenging properties of curcumin, its lower concentrations can activate or inhibit one or more signal transduction pathways in cells. In tumor cells, curcumin can inhibit growth factor-mediated signaling pathways including those coupled to extracellular-regulated kinases and protein kinase C [8-10]. However, phase I clinical trials on Curcumin administered orally, show reduced bioavailability and essentially limited therapeutic effects [11].

In the present study, PLLA (12 % w/w in Chloroform) and Curcumin (0.5 & 1 % w/w based on the weight of PLLA) loaded PLLA were fabricated as nanofibers by electrospinning and evaluated for application as anti-cancer scaffold in the clinical arena. The encapsulation of Curcumin in PLLA nanofibers enables the release of Curcumin in aqueous phase. The *in-vitro* cytotoxicity and cytoproliferative behavior of C-PLLA nanofibrous mat was evaluated using rat C6 glioma and mouse embryonic fibroblasts (NIH 3T3) cell lines. The hydrolysis of PLLA controlled the sustained release of Curcumin. The release rate of Curcumin is strongly controlled by the nanofiber architecture and the enzymes were highly active after the release. The porosity, contact angle measurements and water uptake measurements further confirmed the suitability of the prepared nanofibrous mat for drug delivery application.

Materials and Methods

Materials

Poly L-Lactide (PLLA) (Mw=100,000-150,000), Curcumin, Dulbecco's modified Eagle's medium (DMEM), sodium pyruvate, Fetal Bovine Serum (FBS) and the supplementary antibiotics for tissue culture were purchased from Sigma – Aldrich, India. The rat C6 glioma cells and mouse NIH 3T3 fibroblasts were obtained from the National Centre for Cell Science (NCCS), Pune, India. Chloroform was purchased from Sisco Research Laboratories Private Limited, India. All chemicals were used as received without further treatment or purifications.

*Corresponding author: sheeja@annauniv.edu

Electrospinning Process

The Electrospinning unit used in this experiment has been designed and developed in the Conducting polymer lab, IITM, Chennai. PLLA was dissolved in chloroform and gently stirred continuously for about 2-4 hours. Curcumin was then added to PLLA solution and continuously stirred for 2 hours. The polymer and drug solution was taken in a 2 m*l* syringe to which a needle tip of 0.56 mm inner diameter was attached. The positive electrode of high voltage power supply was connected to the needle and the negative terminal to the drum collector which is covered with aluminium foil as shown in Figure 1. Electric voltage was optimized at 20 kV. PLLA and C-PLLA solutions were electrospun at a flow rate of 0.4 m*l*/hour and the tip to collector distance was kept at 13 cm.

Characterization of Nanofibers

Physico-Chemical Characterization

Porosity Measurements

Percentage Porosity (P) was calculated by comparing its apparent density (ρ) to the bulk density (ρ_0=1.26 g cm^{-3}) according to the equation (1).

$$P = \left(1 - \frac{\rho}{\rho_0}\right) \times 100 \quad (1)$$

Where apparent density (ρ) was calculated according to the equation (2)

$$\rho = \left(\frac{\text{Weight of PLLA nanofibrous mat (g)}}{\text{Length (cm)} \times \text{Width (cm)} \times \text{Thickness of PLLA nanofibrous mat (cm)}} \right) \quad (2)$$

Contact Angle Measurements

The hydrophilicity of the electrospun PLLA nanofiber mat was evaluated by contact angle measurements by placing the sample on the holder of Euromex Optical Microscope equipped with a CCD camera. A drop of deionised water (10 μl) was deposited on the sample surface. The contact angle of the drop oo n the surface was measured at room temperature (27 ^{o}C). Five measurements were performed at different locations and the contact angles were calculated with the help of 'UTHSCSA Image tool' software.

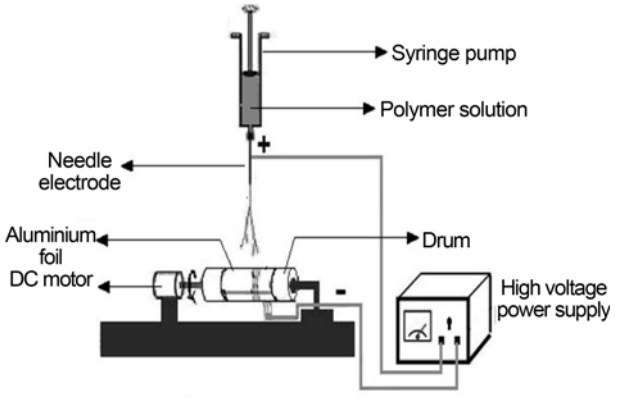

Figure 1. Schematic diagram of electrospinning apparatus.

Water Uptake Test

The water uptake characteristics of PLLA in deionsed water (DW) and phosphate buffered solution (pH = 7.4) were measured. Approximately 5.2 mg of completely dried PLLA nanofibers were weighed and then immersed into 15 m*l* DW and PBS solution respectively. Water uptake study was performed at 37 ^{o}C in an incubator after attaining the equilibrium state. The swollen samples were withdrawn from DW and PBS and weighed after gentle surface wiping with (Whattman No 1) filter paper. The equilibrium water uptake value (WUV) was calculated according to the Eqn. (3) as follows.

$$WUV(\%) = \left(\frac{W_s - W_d}{W_d}\right) \times 100 \quad (3)$$

Where, W_s is the water uptake weight of the PLLA nanofibers at equilibrium and W_d is the dry weight of PLLA nanofibers.

Surface Morphological Studies

The morphology of C-PLLA nanofibers were observed by SEM (FEI Quanta FEG 200 - HRSEM) and TEM (TF 20: Tecnai G2) analysis with an accelerating voltage of 5-20 kV and 200 kV respectively. The diameters of about 100 different fibers were measured by using the UTHSCSA Image tool to obtain their average diameter.

X-ray Diffraction Studies

The crystallinity of the prepared C-PLLA nanofibers was examined using X'pert pro PANalytical Instrument using Cu Kα radiation (λ=1.5418 Å).

Fourier Transform Infrared Spectroscopy

The FTIR spectra were obtained on Perkin-Elmer spectrophotometer RX 100 in the range of 400 cm^{-1} to 4000 cm^{-1}.

Thermal Analysis

The thermogravimetric analysis (TGA) of the fiber was performed by TGA/DTA model SDT 2600. Differential scanning calorimeter was used to determine the glass transition temperature (T_g), crystallization temperature (T_c), melting temperature (T_m), and the degree of crystallinity (X_c) of PLLA and C-PLLA by NETZSCH-Geratebu model DSC 200PC.

Dynamical Mechanical Analysis (DMA)

DMA of PLLA and C-PLLA nanofibrous mat was carried out under stress control mode, where a static stress of 30 kPa was initially applied followed by a dynamic stress of 24 kPa. A temperature scan from 22 ^{o}C to 65 ^{o}C at a heating rate of 4 ^{o}C min^{-1} was applied and nitrogen gas was used as purge.

***In-Vitro* Drug Release Studies**

50 mg of all the formulations was placed in 5 m*l* phosphate buffer solution (PBS) (pH 7.4) containing 10 %

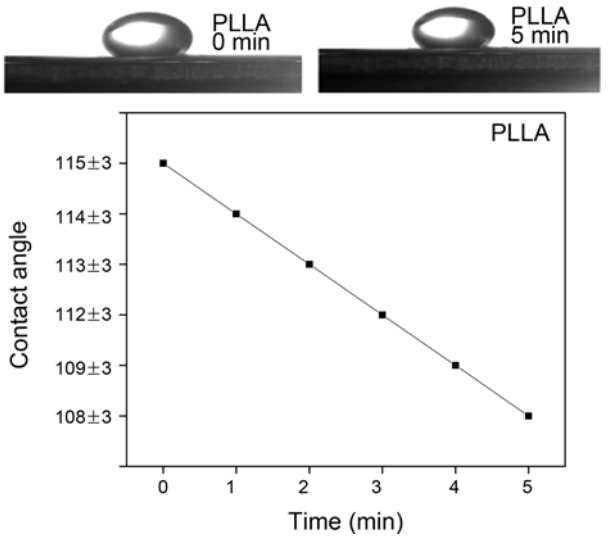

Figure 2. Wettability studies on PLLA nanofibers.

dimethylsulfoxide (DMSO) solution and was incubated in a rotating incubator at 37 °C at 100 rpm. At regular time intervals, one milliliter of aliquot was removed and replaced with same quantity of solution. The amount of Curcumin in releasing media was determined by using HPLC equipped with UV detector at 450 nm.

In-vitro Cytotoxicity

Cell Culture

The rat C6 glioma cells and mouse embryonic fibroblasts (NIH 3T3) were grown and maintained in DMEM containing high glucose and pyruvate, with 10 % fetal calf serum (FCS) supplemented with penicillin (120 units/m*l*), streptomycin (75 mg/m*l*), gentamycin (160 mg/m*l*) and amphotericin B (3 mg/m*l*) at 37 °C in a incubator humidified with 5 % CO_2. Confluent cells were harvested by washing in phosphate-buffered solution (PBS) and followed by trypsinization (0.25 % in 1 Mm EDTA) for subculture. The cell proliferation and viability were measured by the 3-(4,5-Dimethylthiazol-2-yl)-2, 5-diphenyltetrazolium (MTT) assay to determine the amount of the active mitochondrial enzymes present in the viable cells. In this technique MTT was converted in to a coloured (Formazon) product [12].

Experimental Design for Evaluation of Cytotoxicity/ Cytoproliferative Effects

The cytotoxicity and cytoproliferative effects in C-PLLA nanofibrous mat were assessed using C6 glioma and NIH 3T3 fibroblast cell lines. The scaffolds were sterilized by UV treatment before subjecting to the cell culture procedures. The scaffolds were placed in the 96 wells of polystyrene tissue culture plate to observe cellular behavior in them. The cells grown on PLLA nanofibrous scaffold without Curcumin were treated as control. In all culture conditions, the medium was renewed every day and at the end of incubation, the supernatant of each well was replaced with MTT diluted in serum-free medium and the plates incubated at 37 °C for 4 hrs. After aspirating the MTT solution, DMSO was added to each well and pipetted up and down to dissolve all of the dark blue crystals of formazon and then left at room temperature for a few minutes to ensure all crystals are dissolved. Finally, the absorbance was measured using UV spectrophotometer at 570 nm and the corresponding backgrounds at 630 nm were subtracted. The absorbance of the central group was taken as 100 % and the percentage cell viability was recorded by the following equation (4)

$$\% \text{ Cell Viability} = (A_t - A_c / A_c) \times 100 \quad (4)$$

Where A_t is the absorbance of C-PLLA nanofibrous mat with C6 glioma or NIH 3T3 fibroblast cell lines with time and A_c is the absorbance of PLLA nanofibrous mat without Curcumin (control).

Results and Discussion

Physico-Chemical Characterization

The porosity of PLLA nanofibrous mat was 90.2 %. The apparent density and porosity of PLLA nanofibers are shown in Table 1. The contact angle measurements of PLLA nanofibrous mat is shown in Figure 1. The contact angle was 115±3 ° for 0 min which decreased with respect to time as shown in Table 2. The percentage water uptake of PLLA nanofibrous mat in DW and PBS are shown in Figure 3. It was noted that the percentage water uptake was 17.6 % in both DW and PBS media. This low percentage water uptake was due to the hydrophobic nature of the PLLA nanofibrous mat with methyl groups present in the outer surface of fiber. Hence, the ionic content in water did not have any effect on water uptake.

Surface Morphological Studies

The morphology of the electrospun fibers depends on several parameters such as viscosity, conductivity, applied voltage, distance between the needle tip and collector drum, diameter of the needle and the flow rate of the polymer solution. Bead free and uniform nanofibers were obtained from both PLLA and C-PLLA nanofibers. Smooth nano-

Table 1. Apparent density and porosity of PLLA nanofibers

Sample	Weight of PLLA nanofibrous mat (g)	Length x Width of PLLA nanofibrous mat (cm^2)	Thickness of PLLA nanofibrous mat (cm)	Apparent density (g/cm^3)	Calculated average porosity (%)
PLLA	0.0069	2 × 2 = 4	0.014	0.1232	90.2

Table 2. Contact angle measurements of PLLA nanofibers

Time (min)	Contact angles (°)
0	115±3
1	114±3
2	113±3
3	112±3
4	109±3
5	108±3

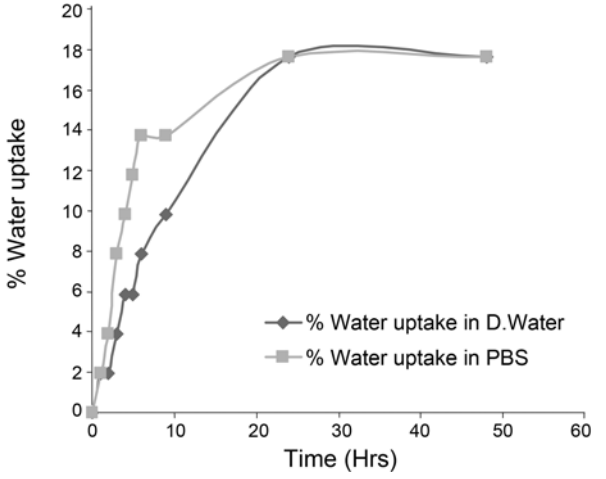

Figure 3. Water uptake test of PLLA nanofibers.

fibers were obtained for C-PLLA nanofibers compared to PLLA nanofibers. The diameter range of PLLA nanofibers and C-PLLA nanofibers was found to be in the range of 50-200 nm respectively. As the concentration of Curcumin increases the diameter of PLLA nanofibers (≈50-100 nm) increased to (≈100-150 nm) as shown in Figures 4(a), (b) and (c). The dispersed Curcumin in PLLA was visible as black spots in the TEM image of a single nanofiber of C-PLLA as shown in Figure 4(d). The histogram peaks are shown in Figure 4(e). The crystallinity of PLLA and C-PLLA was determined by XRD. The XRD profiles are shown in Figure 5. The diffraction pattern of PLLA showed a characteristic peak at 2θ=16.9 °. The diffraction peaks for Curcumin are reported at 8.43 °, 11.76 °, 14.14 °, 16.91 °, 17.87 °, 20.80 °, 23.10 °, 24.21 °, 25.24 °, 26.98 °, 27.86 ° and 28.65 ° [13]. On the other hand, C-PLLA showed only a broad peak stretching between 15-26 °, centered at about 2θ=20 °, characteristic of amorphous Curcumin phase after incorporation into PLLA [14]. The FTIR spectra of PLLA and C-PLLA nanofibrous mat are shown in Figure 6. The peak at 1601 cm^{-1}, 1626 cm^{-1} and 1511 cm^{-1} were attributed to the stretching vibration of C=C. The olefinic stretching frequency in Curcumin was found in the C-PLLA spectrum, which was absent in the PLLA nanofibers. This confirmed the presence of Curcumin in the C-PLLA nanofibrous mat. The other characteristic peaks of PLLA and C-PLLA nanofibers revealed similar structure and are given in Table 3 [15].

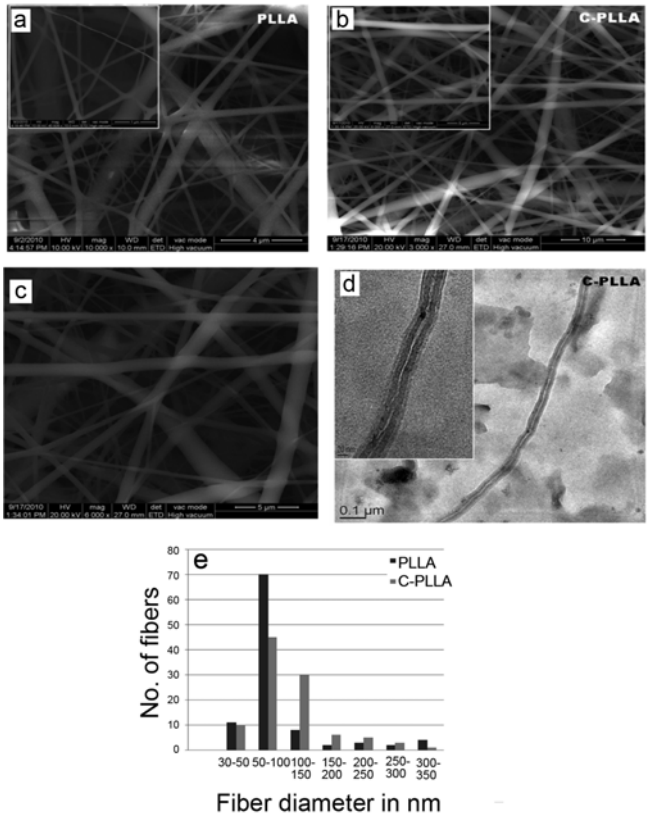

Figure 4. SEM images of (a) PLLA nanofibers, (b) C-PLLA nanofibers (0.5 wt %), (c) C-PLLA nanofibers (1 wt %), (d) TEM image of C-PLLA single nanofiber, and (e) Histogram graph of PLLA and C-PLLA nanofibers.

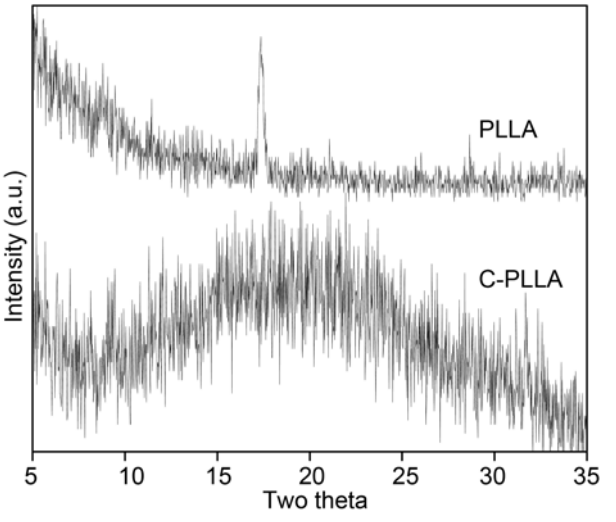

Figure 5. XRD graph of PLLA and C-PLLA nanofibers.

Thermal and Mechanical Properties

The TGA graph of PLLA and C-PLLA nanofiber mats are shown in Figure 7. The weight loss below 100 °C was due to evaporation of solvent and water. The decomposition tem-

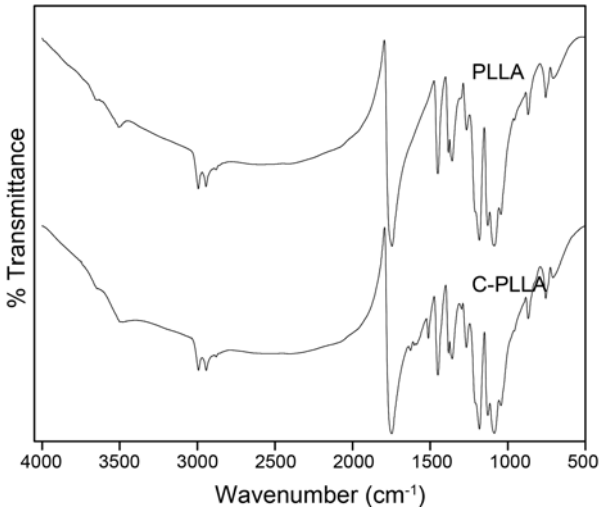

Figure 6. FTIR spectra of PLLA and C-PLLA nanofibers.

Table 3. FTIR spectra of PLLA and C-PLLA peak band assignments nanofibers

Peak position (cm^{-1})	Assignment
3507	-OH stretch (free)
2993 (asymmetric), 2943 (symmetric)	-CH- stretch
1746	-C=O carbonyl stretch
1450	$-CH_3$ bend
1381, 1358	-CH- deformation including symmetric and asymmetric bend
1265	-C=O bend
1183, 1128, 1086	-C-O- stretch
1044	-OH bend
925, 868	-C-C stretch

perature of PLLA was 330 °C whereas C-PLLA was 294 °C. The higher decomposition temperature of PLLA shifted to lower temperature in C-PLLA nanofibers thus confirming Curcumin conversion to amorphous form. The amorphous form of the drug dispersed in the polymer matrix has the benefit of increasing the aqueous solubility and thus the bioavailability of low water soluble drugs. The DSC graph of PLLA and C-PLLA nanofiber mats are shown in Figure 8. The T_g, T_m and Xc (degree of crystallinity) values of PLLA and C-PLLA (0.5 % and 1 %) are presented in Table 4. The T_g value increased slightly on the addition of Curcumin to PLLA which established better association in the C-PLLA nanofibrous mat than that of PLLA nanofibrous mat due to the presence of phenolic OH groups and keto groups in Curcumin. Though the difference in T_g was significant, the melting points were nearly the same, and the enthalpy change corresponding to melting was very much different.

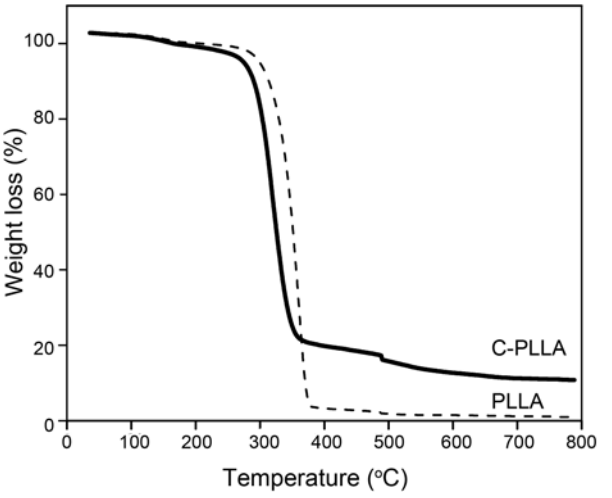

Figure 7. TGA graph of PLLA and C-PLLA nanofibers.

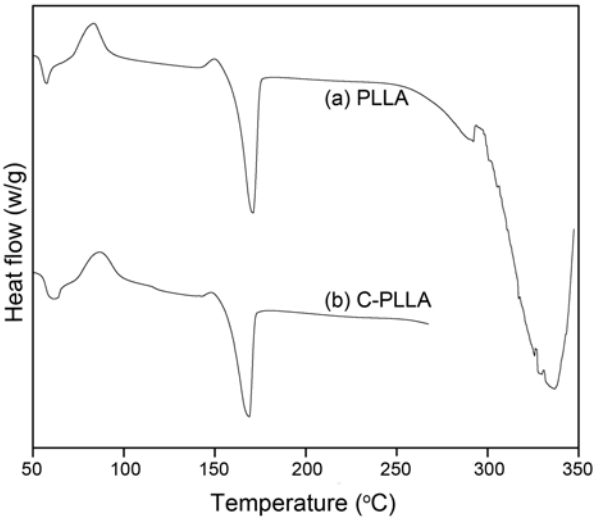

Figure 8. DSC graph of (a) PLLA and (b) C-PLLA nanofibers.

Hence, as a result of loaded Curcumin, the interchain interaction reduced. Since, melting is influenced by the crystallinity, decreasing melting point suggested a decrease in crystallinity of PLLA, as a result of Curcumin loading. The viscoelastic parameters of storage modulus (E'), loss modulus (E") and tan δ as a function of temperature were determined using DMA analysis and the results are shown in Figure 9. The capabilities of the PLLA and C-PLLA nanofibrous mat to store energy during deformation are expressed in terms of storage modulus which represents the elastic component of a material. Loss modulus gives the amount of energy dissipated as heat. Tan δ is the ratio of loss to storage modulus and it indicates how much energy is lost due to damping. The storage modulus, loss modulus and tan δ values of PLLA and C-PLLA are presented in Table 5.

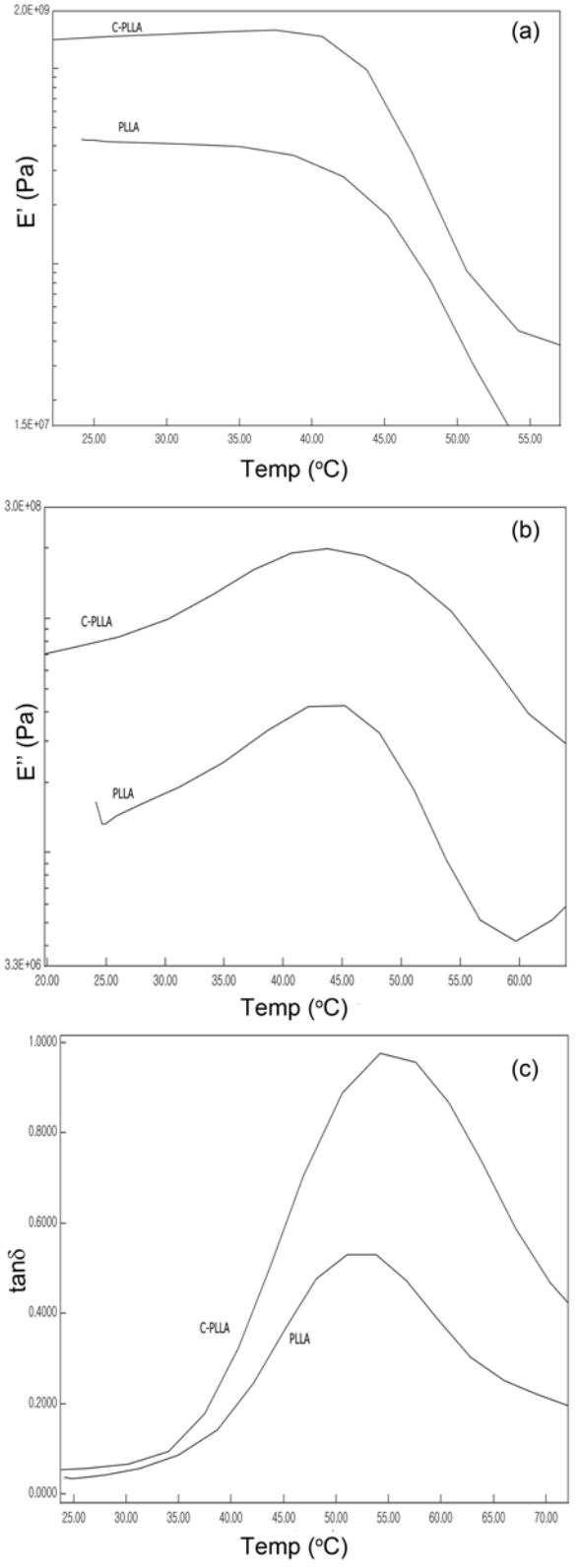

Figure 9. DMA curves of (a) Storage modulus (b) Loss modulus and (c) Tan delta of PLLA and C-PLLA nanofibers.

Table 4. Thermal properties of the PLLA and C-PLLA nanofibers

Sample	T_g (°C)	T_m (°C)	H_f (J/g)	X_c (%)
PLLA	57.41	170.94	66.61	32.7
C-PLLA (0.5 wt %)	61.80	170.12	52.16	25.6
C-PLLA (1 wt %)	65.18	171.2	34.32	16.8

Table 5. Mechanical properties of the PLLA and C-PLLA nanofibers

Sample	Storage modulus (Pa)	Loss modulus (Pa)	Tan δ
PLLA	3.3×10^8	4.2×10^7	0.8956
C-PLLA	1.6×10^9	2×10^8	1.1041

In-vitro Drug Release Studies and Cytotoxicity Studies

The rate of release of Curcumin from the PLLA nanomesh is dependent on two main factors, viz, the thickness of the C-PLLA nanomesh, and the rate at which PLLA degrades and allows for the optimization of Curcumin release within the body. In general drugs can be released in a controlled manner with first order kinetics. In the present study, the feasibility and potential of PLLA nanofibrous scaffolds as a drug delivery vehicle for Curcumin release was investigated. The in vitro release of Curcumin into PBS containing DMSO over a period of 8 days is shown in Figure 10. The C-PLLA nanoscaffolds showed controlled and sustained release of Curcumin (i.e. 81-86 % release) in 8 days. At the initial stage, there was small burst effect which could be due to the release of some loosely bound Curcumin on the surface. This loosely bound Curcumin might be released by a mechanism of diffusion through the aqueous pores on the surface created by the water uptake by nanoscaffolds immediately after being exposed. At the later stage, the Curcumin release was slow, whose rate was determined by the diffusion of PBS into the PLLA matrix, because the release of Curcumin from C-PLLA nanofibers depended

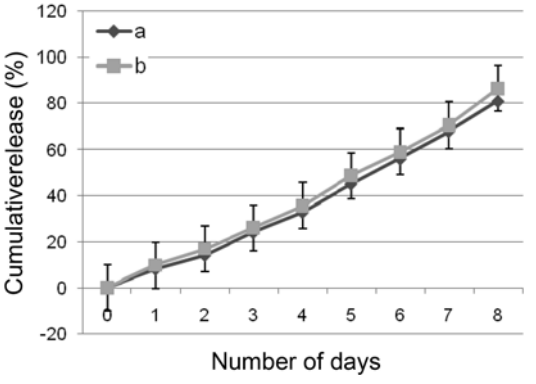

Figure 10. Drug release studies for (a) C-PLLA (0.5 wt %) (b) C-PLLA (1 wt %) nanofibrous scaffolds.

upon the diffusion path filled up by PBS. In other words, the hydrophobic nature of PLLA could have delayed PBS penetration; hence, the diffusion of the Curcumin into the release medium was retarded, which resulted in a small burst effect. Curcumin was then released more slowly once the PBS was filled in the diffusion path length, after which the release rate was determined not by the erosion of PLLA but by the diffusion of Curcumin in the PLLA matrix due to low degradation of PLLA. This initial small burst Curcumin release was later followed by more controlled and sustained release. The percentage cumulative Curcumin release at the end of 8 day period for 0.5 and 1.0 wt % formulations was 81.4±1.3 and 86.7±1.7 % respectively. No significant difference in release was observed between nanoscaffolds containing 0.5 wt % and 1.0 wt % Curcumin in the conducted release period. Nanoscaffolds formulated drugs and their in-vitro release profile helped to understand the behavior of these systems in terms of drug release, and therefore its efficacy.

In-vitro cytotoxicity studies of the scaffolds were performed by MTT assay, a colorimetric method in which the absorbance (OD values) of Formazon reflects the number of viable cells. Using MTT assay, the cellular metabolic activity was monitored which measures the activity of

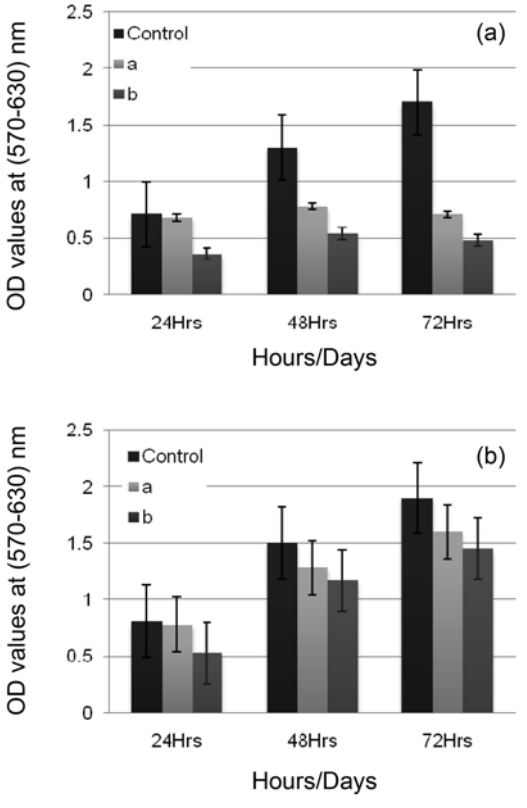

Figure 11. MTT assay for (A) C-PLLA (0.5 wt %) (B) C-PLLA (1 wt %) nanofibrous scaffolds using C6 glioma cells (a) and NIH 3T3 fibroblasts (b).

mitochondrial dehydrogenase, which identifies the number of cells in an active metabolic state. The proliferation rate of C6 glioma and NIH 3T3 fibroblasts on PLLA (control) and C-PLLA with 0.5 wt % and 1 wt % ratios is shown in Figure 11. In the current study it was found that the extent of cellular proliferation on PLLA nanofibrous scaffolds with or without Curcumin were significantly altered as shown in the MTT assay graph. It was found that the cell densities were lower after administration of Curcumin into PLLA nanofibers as compared to control after 24, 48 and 72 h.

Cell attachment, proliferation and differentiation depend on the cell type and microenvironment of the cells such as matrix nature. The cellular proliferation on PLLA was affected due to difference in nature of cells and the presence of Curcumin in different concentrations. Inhibitory effects of the Curcumin were observed in both the formulations and the cell lines used, as Curcumin inhibit NF-κB which in turn force the cells to enter apoptotic pathways but after 72 h the viability of fibroblasts was high at both concentrations in comparison to the viability obtained at 24 h. However, in comparison to control these were always less. In contrast, Curcumin was found to have more inhibitory effect on C6 glioma cells where around 60 to 80 % drop in viability was observed while around 85 to 76 % of fibroblasts were viable at the end of 72 h. As the culture medium was changed every day, along with the medium, the Curcumin might have leached out which resulted in lower concentration of available Curcumin for the cells. Low doses of Curcumin stimulated the proliferation of mouse embryonic fibroblasts (NIH 3T3) whereas high doses inhibited it. A study on mouse lymphocytes reported that a low-dose Curcumin increased the proliferation of splenic lymphocytes, whereas high-dose Curcumin depressed it indicating its ability to differentially regulate the proliferation of splenic lymphocytes [16].

Low doses of Curcumin stimulated proliferation, possibly because of the effect of Curcumin on the cell signaling pathways. This could occur if Curcumin stimulated the induction of Phase II (proliferation phase) defense genes, which would enhance cell survival and have a beneficial effect on homeostatic responses. This, in turn, would stimulate cell proliferation. Also, it is possible that low doses of Curcumin may reduce the production of Interleukin-8 (IL-8), thus reducing inflammation. High doses of Curcumin, however, may potentially stimulate apoptosis, or cell death, due to the activation of caspase pathways. As a result, it would inhibit cell proliferation. The difference in the behaviour of the Curcumin towards the cell types, time and concentration dependent cell viability would be attributed due to the multi-mode action of Curcumin. Curcumin can interfere with the activity of the transcription factor NF-κB, which has been linked to a number of inflammatory diseases such as cancer. Curcumin may inhibit mTOR complex I *via* a novel mechanism and it modulates growth of tumor cells through regulation of

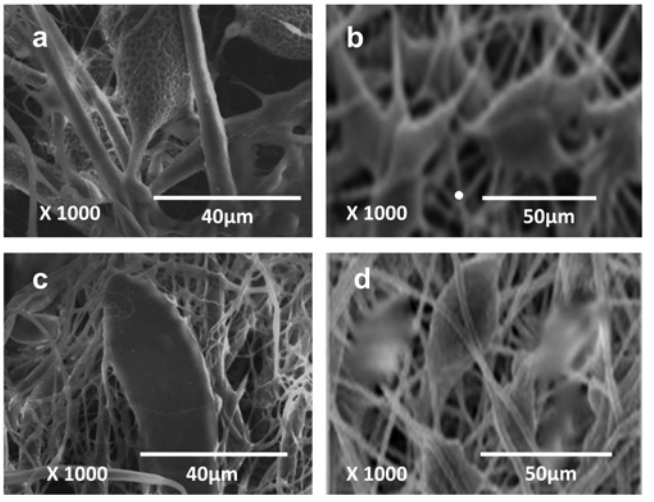

Figure 12. SEM photographs (at 1000X & C at 5000X) of C6 glioma cells (a) and NIH 3T3 fibroblast (b) grown on PLLA nanofibrous scaffolds; and C6 glioma cells (c) and NIH 3T3 fibroblast (d) grown on C-PLLA nanofibrous scaffolds.

multiple cell signaling pathways [17,18].

Although, Curcumin has potential anticancer effects which stem from its ability to induce apoptosis in cancer cells without cytotoxic effects on healthy cells, in the present study it was found to have inhibitory effect on the normal cell line used (NIH 3T3 fibroblasts), although the degree of inhibition was very much less than C6 glioma cells. The current observation proves that Curcumin formulation with PLLA nanofibrous scaffolds can be used for cancer therapy such as breast, colon, skin etc.

Similar patterns were observed from the SEM analysis supporting the data of MTT assay. The SEM photographs showed that the C6 glioma cells (Figure 12(a)) and fibroblasts (Figure 12(b)) grew very well over PLLA nanofibrous scaffolds and the shapes of the same were maintained during the culture period. Cells grew in the direction of the fiber orientation according to the architecture of the nanofibrous structure and some cells migrated underneath the fibers. The C6 glioma cells grown on C-PLLA nanofibrous scaffolds (Figure 12(c)) were less dense than the fibroblasts (Figure 12(d)). The MTT assay and SEM analysis supported the observation that C-PLLA nanofibrous scaffolds could be considered as a good biocompatible scaffold for therapeutic anti-cancer drug delivery.

Conclusion

Beadless, smooth, uniform C-PLLA nanofibers were produced by electrospinning method. The percentage porosity, water uptake, contact angle measurements, cytotoxicity and *in-vitro* drug release confirmed the controlled drug release of Curcumin thus making C-PLLA a promising scaffold for drug delivery. Further, the *in-vitro* drug release and cytotoxicity studies confirmed C-PLLA nanofibrous scaffold as a promising substratum for anti-cancer drug delivery applications.

Acknowledgement

The authors acknowledge the Department of Science and Technology (DST) for financial assistance (Project No. SR/S1/PC-56/2009 (G) dated 12.07.2011).

References

1. Z. M. Huang, Y. Z. Zhang, M. Kotaki, and S. Ramakrishna, *Compos. Sci. Techol.*, **63**, 2223 (2003).
2. S. Bibekananda, V. Subramanian, T. S. Natarajan, X. Rong-Zeng, C. Chia-Cheng, and F. Wun-Shain, *Appl. Phys. Lett.*, **84**, 1222 (2004).
3. J. S. Travis and A. V. R. Horst, *Biomater.*, **29**, 1989 (2008).
4. A. Anitha, V. G. Deepagan, R. Divya, M. Deepthy, S. V. Nair, and R. Jayakumar, *Carbohyd. Polym.*, **84**, 1158 (2011).
5. L. T. Rajesh, S. Anuj, and R. K. Maheswari, *The AAPS J.*, **8**, E443 (2006).
6. A. J. Ruby, G. Kuttan, K. D. Babu, K. N. Rajasekharan, and R. Kuttan, *Cancer Lett.*, **94**, 79 (1995).
7. S. Shishir, S. Gautam, and B. Aggarwal Bharat, *Annals of the Newyork Academy of Sciences*, **1056**, 206 (2005).
8. A. Duvoix, R. Blasius, S. Delhalle, M. Schnekenburger, F. Morceau, E. Henry, M. Dicato, and M. Diederich, *Cancer Lett.*, **223**, 181 (2005).
9. H. W. Suh, S. Kang, and K. S. Kwon, *Molecular and Cellular Biochem.*, **298**, 187 (2007).
10. J. K. Lin, *Advances in Experimental Med. Biol.*, **595**, 227 (2007).
11. B. A. Bharat, K. Anushree, and A. C. Bharti, *Anticancer Res.*, **23**, 363 (2003).
12. T. Mossmann, *J. Immun. Methods*, **65**, 55 (1983).
13. D. Franscesco, W. Yuwen, J. Li, and Q. Huang, *J. Agricultural and Food Chem.*, **58**, 2848 (2010).
14. J. Shaikh, D. D. Ankola, V. Beniwal, D. Singh, and M. N. V. Ravikumar, *Eur. J. Pharmaceutical Sci.*, **37**, 223 (2009).
15. Y. Chen, J. Lin, Y. Fei, H. Wang, and W. Gao, *Fiber. Polym.*, **11**, 1128 (2010).
16. G. C. Jagetia and B. B. Aggarwal, *J. Clin. Immun.*, **27**, 19 (2007).
17. J. Ravindran, S. Prasad, and B. B. Aggarwal, *AAPS J.*, **11**, 495 (2009).
18. B. A. Bharat, Y.-J. Surh, and S. Shishir, Springer Science + Business Media, LLC, 223 Spring Street, New York 10013, USA, 2007.